NACA RM 57E17

NACA

RESEARCH MEMORANDUM

EXPERIMENTAL INVESTIGATION OF CREEP BENDING AND BUCKLING OF THIN CIRCULAR CYLINDRICAL SHELLS

By Burton Erickson, Sharad A. Patel, Francis W. French, Samuel Lederman, and N. J. Hoff

Polytechnic Institute of Brooklyn

NATIONAL ADVISORY COMMITTEE
FOR AERONAUTICS

WASHINGTON

July 23, 1957

NACA RM 57E17

NATIONAL ADVISORY COMMITTEE FOR AERONAUTICS

RESEARCH MEMORANDUM

EXPERIMENTAL INVESTIGATION OF CREEP BENDING AND BUCKLING OF THIN CIRCULAR CYLINDRICAL SHELLS

By Burton Erickson, Sharad A. Patel, Francis W. French, Samuel Lederman, and N. J. Hoff

SUMMARY

Forty-three cylinders of 40-inch length and 16-inch diameter, made of 5052-0 aluminum-alloy sheets of 0.032-, 0.040-, 0.051-, and 0.064-inch thickness, were subjected to bending moments constant along the cylinder and in time in an oven which maintained a constant temperature of 500° F during the test. All the cylinders failed by buckling. The time that elapsed between load application and collapse was measured.

INTRODUCTION

It is known that airplanes flying at supersonic speeds are heated by the airstream. Since the structural elements of these planes have to carry loads, they are simultaneously subjected to stresses and to high temperatures. Under such conditions the elements show deformations increasing with time even if the loads are constant. This behavior is termed creep.

When creep is present in a structure, the distribution of the stresses in it differs from that in a perfectly elastic structure that follows Hooke's law. In addition, creep causes new modes of instability to appear, and the structure is likely to collapse after some time even though it is perfectly capable of carrying the loads for a shorter period. Since creep laws are complex, until now it has been possible to develop theories for the effects of creep only for simple structural arrangements; in particular, trusses, frames, and columns have been studied.

Since thin shells are at least as important as trusses and frames in an airplane structure, an experimental investigation into the failure of thin circular cylindrical shells subjected to constant bending moments

at elevated temperatures was undertaken at the Polytechnic Institute of Brooklyn. The present report is a description of the test equipment used and of the results obtained with 43 test specimens. The cylinders failed by buckling, and their lifetime depended greatly on the difference between the applied bending moment and the critical moment at the test temperature.

The investigation was carried out at the Polytechnic Institute of Brooklyn under the sponsorship and with the financial assistance of the National Advisory Committee for Aeronautics.

SYMBOLS

d_1, d_2, d_3	deflections shown in figure 7
E	Young's modulus
h	wall thickness of cylindrical shell
I	moment of inertia of cross section of cylinder
L	length shown in figure 7
l_1, l_2	lengths shown in figure 7
M	bending moment
n	creep exponent in steady creep law for tension
r	radius of cylinder
t	time, min
ΔD	change in length of vertical diameter of cylinder
δ	vertical displacement of point of intersection of axis with end plane of cylinder
$\dot{\epsilon}$	tensile creep strain rate
η	axial displacement of point of intersection of axis with end plane of cylinder
θ	rotation of end plane of cylinder

$\dot{\theta}$ rate of end rotation

$\dot{\kappa}$ rate of change of curvature of axis of cylinder

λ,μ constants in creep formulas

φ angle measured from vertical in plane perpendicular to axis of cylinder

σ stress

Subscripts:

cr critical

max maximum

TEST APPARATUS

The main parts of the test apparatus are a lever loading mechanism for maintaining a constant bending moment on the cylinder, a rigid support for the cylinder, and an oven capable of producing a constant elevated temperature in the cylinder. Details of the apparatus are given in the following discussion.

Loading Device

The constant bending moment is applied to the cylinder by means of a horizontal lever in the shape of a long thin isosceles triangle (fig. 1). Dead weights are hung at the apex of the triangle from a fixture which rests with a knife edge in a hardened V groove. A horizontal steel link connects each end of the base of the triangle to a heavy steel ring (fig. 2) inside the oven. The test cylinder is secured to this ring by two rows of circumferential clamps. A similar steel ring is used to fasten the other end of the test specimen to a heavy attachment cylinder mounted on a massive strongback (fig. 3).

The weight of the steel end ring, its bolts, and its attachments, as well as half the weight of the two steel links, is counterbalanced by the weight suspended from the horizontal beam that is pivoted in the middle of the vertical leg of the isosceles triangle (fig. 1). All the vertical forces of the system are finally transferred from the castored base plate of the loading device to the supporting structure; thus no shear force is transmitted to the test cylinder. The pure bending moment applied to the cylinders is the weight suspended from the apex of the

loading triangle times the distance from the apex to the pivot in the middle of the base of the triangle (fig. 1) plus the weight of the loading triangle times the distance of its center of gravity from the pivot.

Oven

The oven was designed to produce constant temperature in the specimen throughout the temperature range of 150° to 1,000° F with a tolerance of ±1° F. It was constructed in four moveable sections (fig. 4). Each section is mounted on wheels set in tracks laid parallel on either side of the strongback structure. To facilitate mounting of the cylinder, attachment of thermocouples, and other necessary preliminaries to a test, the sections can be moved away from the strongback. When these preparations for the test are completed, the oven sections are returned and clamped in place around the specimen.

The total internal volume of the oven is 54 cubic feet. The internal dimensions are 52 inches (length), 46 inches (height), and 37 inches (width). The interior facing is $\frac{1}{2}$-inch-thick Transite sheet bolted to a steel angle-section frame. A 2-foot layer of 85-percent-magnesia block insulation encases the heating chamber. A facing of $\frac{1}{2}$-inch-thick Transite sheet bolted to a steel angle-section frame forms the outside surface (fig. 5). Structural connection between the inner and outer frames is made by $\frac{1}{2}$-inch-thick Transite tie plates (fig. 6). Mating faces of each of the moveable sections are stepped to minimize heat loss at the junctions.

The power necessary to bring the test chamber to 500° F in approximately 1 hour was calculated to be about 30 kilowatts. The power required to maintain this temperature against conduction losses after the test temperature had been attained was determined to be of the order of 6 to 7 kilowatts. The oven is heated by 128 two-way strip heaters with a maximum power rating of 32 kilowatts. The strip heaters are arranged in 3 individually controlled banks, 40 along the oven bottom, 48 along the sides, and 40 along the top. The two-way strip heater is a resistance element with a center tap. By connecting the power across the center tap and the two end terminals (parallel), maximum output is achieved. This arrangement is used for the initial stage of heating from room temperature by direct connection of the heaters to a power source. When the oven temperature becomes sufficiently high, automatic stepless controllers are switched into the circuit. The controllers are connected across the end terminals of the heaters (series), thus reducing the controlled power to one-quarter of the rated power or 8 kilowatts. While this procedure requires some alertness on the part of the testing crew, it is considerably more economical than full power control.

The stepless controller supplied by the West Instrument Corp. of Chicago, Illinois, is essentially a pyrometer controller combined with a saturable core reactor.

Temperature control is accomplished by three thermocouples, one for each of the three banks of heaters mentioned. To maintain an even distribution of heat throughout the oven, it is necessary that all heaters function properly. For this reason, each individual heater is connected to an indicating lamp. If any of the heaters has open circuits, the light immediately indicates the malfunction.

Conduction losses through the strongback are compensated for by one 1,000-watt tubular heater on the cylinder clamping ring, one 1,000-watt tubular heater inside the strongback attachment cylinder, and two 1,000-watt immersion heaters secured to the supporting legs of the strongback attachment cylinder. Conduction loss through the load linkage is compensated by one 1,000-watt tubular heater on the front cylinder clamping ring. The compensating heaters are manually controlled through powerstats.

Temperature Measurement

Temperatures were measured at nine points on the specimen. Iron-constantan thermocouples were tied with copper wire to the specimen in a manner to insure that the junctions remained in close contact with the surface at all times. The thermocouples were wired to a selector switch connected to a No. 1117 Brown indicating potentiometer. The temperatures at the nine points were read consecutively.

Of the points surveyed three were at the front end of the cylinder, three halfway between the ends, and three at the rear end. In each of the three planes one thermocouple was located at the top, one at the bottom, and one on the horizontal diameter of the cylinder. The control points for the automatic temperature regulation were halfway between the two ends of the cylinder.

Measurement of Deformations

The deformations measured were:

(1) Rotation of the end plane of the cylinder θ

(2) Vertical displacement of the point of intersection of the axis of the cylinder with the end plane δ

(3) Longitudinal displacement of the point of intersection of the axis of the cylinder with the end plane η

(4) Change in vertical diameter in a plane perpendicular to the axis of the cylinder and bisecting the cylinder ΔD

When the first three of these deflection quantities were measured, use was made of the geometry of the loading linkage to transmit the motion of points in the end plane of the cylinder to the outside, where measurements could be made at room temperature. Measurements were then made of the strains produced in thin, cantilever-beam dynamometers by the motion of the loading linkage. The strains, as read on a Baldwin strain indicator, were calibrated against the deflection of the end of the beams so that by reading the strains one could find the beam deflections and thence the cylinder deflections from the geometry of the system (fig. 7). In each particular case this was done as follows:

To measure θ, one end of a cantilever beam of length l_1 was clamped in a vertical position to the upright of the castored base plate that acts as a fulcrum for the counterbalancing beam. The other end of the cantilever was set against the base of the loading triangle. From the geometry of the linkage it is seen that

$$d_1/l_1 = \tan \theta \approx \theta \tag{1}$$

where d_1 is the deflection of the end of the cantilever beam.

To determine δ, one end of a cantilever beam of length l_2 was clamped in a horizontal position to the upright of the base plate. The other end of the cantilever was set against the counterbalancing beam. From the geometry it is seen that

$$\delta = \left(L/l_2\right)d_2 \tag{2}$$

where d_2 is the deflection of the end of the cantilever and L is the length of the counterbalancing beam from the fulcrum to the center of the cylinder end plane.

For determining η, one end of a cantilever beam was bolted to the supporting structure on which the base plate rests. The other end was set against the edge of the castored base plate. In this case

$$\eta = d_3 \tag{3}$$

where d_3 is the deflection of the end of the cantilever.

Measurements made in the first few experiments indicated that the magnitude of η was small compared with that of θ and δ and in subsequent tests only the latter two quantities were measured.

The change in diameter was measured by means of a high-temperature linear variable differential transformer made by the Schaevitz Engineering Co. of Camden, New Jersey. The stationary transformer coil was suspended from the upper surface inside the cylinder. A long slender rod was attached to the transformer core and the assembly was placed inside the coil with the end of the shaft resting on the bottom surface of the cylinder so that the assembly could move freely in a vertical direction. The relative motion between the core and coil as a result of the cylinder flattening changed the output of the transformer. The change in output voltage was calibrated to give the change in diameter. A graphical record of the change in diameter with time was obtained with the aid of a Brown "Electronik" recorder made by the Minneapolis-Honeywell Regulator Co. Measurements of the change in diameter indicated that this quantity was small compared with the other deformations measured.

DESCRIPTION OF TESTS

Test Specimens

All specimens tested were made of 5052-0 aluminum-alloy sheets with thicknesses of 0.032, 0.040, 0.051, and 0.064 inch. The sheet was rolled into a cylinder 16 inches in diameter and 48 inches long with a $1\frac{1}{4}$-inch overlap at the line of juncture. AN430AD4 rivets spaced $\frac{1}{2}$ inch apart closed the cylinder. Steel clamping rings with 16-inch inside diameter, 1 inch thick and 4 inches long with $\frac{1}{2}$- by $2\frac{3}{4}$-inch flanged ends were slipped over the ends of the cylinder. Two circumferential rows of $\frac{5}{8}$-inch-diameter holes $1\frac{1}{4}$ and 3 inches from the end of the ring were provided to take through bolts for drawing 24 knurled-faced convex clamps in two rows against the inside surface of the cylinder and to secure in this manner 4 inches of the end of the cylinder within a steel ring at each end.

The flanged portion of the rear clamping ring contains a circumferential set of holes which are matched to studs protruding from the strongback. The cylinder was secured in place on these studs, forming a cantilever clamped to the strongback.

The load links and the counterbalance beam are attached to a vertical fitting consisting of two steel bars $\frac{1}{2}$ inch by 3 by 21 inches spaced $1\frac{1}{4}$ inches apart and welded to the front face of the front clamping ring

and extending across the entire diameter of the ring (fig. 2). The loading links are pinned to the ends of the fitting by means of 1-inch-diameter hardened steel pins, while the counterbalancing beam is pinned to the midpoint. The center-to-center spacing of the end holes is 18 inches; the third hole is exactly halfway between the ends.

Test Procedure

With the test specimen securely mounted, the thermocouples were tied in place. The clamping-ring heaters were positioned and connected, and the oven was rolled into place around the specimen and sealed. The load links were connected to the lever, and the counterbalancing beam was pinned and weighted. A hydraulic jack was placed under the apex to support the end of the loading lever, and the dead-weight load was applied. At this stage of the test, the entire weight was supported by the jack.

Switches were thrown and full power was fed to all heaters. As the temperature of the oven increased, a careful check was maintained at each of the nine instrumented points. Some points naturally approached the test temperature more quickly than others. As the test temperature was reached at these points, the corresponding heaters were cut back to maintain it. Stabilized test temperature was reached in $1\frac{1}{2}$ to 2 hours and was maintained therefrom with a maximum variation of $\pm 1^{\circ}$ F for the remainder of the test.

When the temperature had been stabilized, the load was applied. This was accomplished by opening the metering valve of the hydraulic jack and allowing the full force of the load to be smoothly transferred from the jack to the end of the lever. The operation consumed about 10 seconds of time. The time to failure of the cylinder was measured from the instant of full load application.

To measure changes in the length of a vertical diameter, the differential transformer was placed on the cylinder and electrically connected to the Brown Recorder. A long, thin wire was attached to the transformer core for calibration purposes and carried through an aperture in the oven wall to the outside. The oven was then closed and power was fed to the heaters. To measure the remaining three deformation quantities, the three dynamometers were positioned and connected to strain indicators while the oven was heating. When the oven was fully stabilized at the test temperature, the transformer was calibrated by displacing the free end of the wire known amounts with a micrometer feed and by noting the corresponding readings on the recorder. The recorder was set in motion and the load applied. The strain indicators were read at regular time intervals until the cylinder buckled and the time required for buckling was noted.

PRESENTATION AND DISCUSSION OF RESULTS

The main results of the experiments are collected in table 1. Of the 43 cylinders tested, 10 were loaded "statically." This term means that the loads were increased from zero to the value at which the cylinder collapsed as is usual in routine static testing. The buckling moments at collapse are listed in the table.

Table 2 repeats this experimental information for the static-test cylinders and compares it with the predictions of theory. On the assumption of perfectly elastic behavior the following formula was derived in reference 1 for the maximum stress in a bent cylinder at the moment of collapse:

$$\sigma_{cr_{max}} = 0.35E(h/r) \tag{4}$$

where E is Young's modulus, h, the wall thickness, and r, the radius of the cylinder. Except for the numerical constant, this formula is the same as the one generally used for the calculation of the buckling stress of axially compressed thin circular cylinders. The critical bending moment is obtained from equation (4) if the stress is multiplied by $I/r = \pi r^2 h$. The result is

$$M_{cr} = 1.1Erh^2 \tag{5}$$

The values of this critical bending moment are also given in table 2, as well as the ratios of the experimental moments to the theoretical moments. The average ratio is 0.614.

The deviation between the experimental and the theoretical values is less than that found with cylinders subjected to uniform axial compression. There the theoretical coefficient obtained from the small-deflection theory is 0.6 while the experimental values range between 0.09 and 0.36 (see ref. 2). Nevertheless, the comparison between the experimental results of the present test series and the theory is not entirely justifiable because the deformations were not purely elastic. In the room-temperature tests the maximum stresses calculated from elastic theory ranged between 8,090 and 14,480 psi; in the tests carried out at 500° F, the corresponding values were between 6,790 and 11,110 psi. In comparison, the ultimate and the yield stresses of the material were approximately 28,000 and 11,500 psi at room temperature and 7,500 and 7,000 psi at 500° F. Some inelastic deformation was likely to occur above 7,500 psi at room temperature and above 3,000 psi at 500° F. The values of the modulus were about 10.5×10^6 and 8×10^6 psi at the two temperatures mentioned.

For a satisfactory comparison between theory and experiment the plastic deformations of the material should be taken into account. For the time being this is not possible for two reasons: First, no theory has yet been developed for the buckling of cylinders in the inelastic range when the loading consists of constant bending moments; and, secondly, no reliable tangent-modulus values are available for the material at 500° F.

As far as the creep-buckling tests are concerned, the basic information is the critical time listed in table 1 and the plots of vertical end displacement and of end rotation against time. The latter were obtained for cylinders 15 to 43; three such plots are reproduced here in figure 8. Each curve shows an instantaneous, elastic or elastic-and-plastic deformation at the moment of load application. This is followed by a short, slightly curved line attributable to primary creep and to the interaction between elastic and creep deformations. The major portion of each diagram is taken up by the straight lines corresponding to steady creep, and before collapse the experimental lines curve up rapidly in consequence of the instability of the structural deformations.

From the straight-line portion of the curve the steady rate of change $\dot{\theta}$ of the end rotation was determined for each cylinder. This value was then plotted against the applied moment on logarithmic paper. Figure 9 contains these plots for the wall thicknesses $h = 0.032$, 0.040, and 0.051 inch. The figure shows that a straight line can be passed through the experimental points without an undue amount of scatter. The slope of the line is the creep exponent n in the steady creep law for tension

$$\dot{\epsilon} = (\sigma/\lambda)^n \tag{6}$$

where $\dot{\epsilon}$ is the strain rate in tension, σ the tensile stress, and λ a constant, as well as in that for bending

$$\dot{\kappa} = (M/\mu)^n \tag{7}$$

where $\dot{\kappa}$ is the rate of change of the curvature of the axis of the cylinder, M is the applied bending moment, and μ is a constant. In the tests here described the connection between $\dot{\kappa}$ and the rate of rotation $\dot{\theta}$ of the end of the cylinder was

$$\dot{\kappa} = \dot{\theta}/L = \dot{\theta}/40 \tag{8}$$

Finally, the value of λ was determined from the test data with the aid of the formula

$$\lambda = \frac{\left(M/4hr^2\right)}{(r\dot{\kappa})^{1/n} \int_0^{\pi/2} (\cos \varphi)^{(n+1)/n} \, d\varphi} \tag{9}$$

where r is the radius of the thin cylinder and φ is the angle measured from the vertical in the plane perpendicular to the axis of the cylinder. Equation (9) was derived in reference 1.

Table 3 gives the values of the creep constants. No values are given for the 0.064-inch-thick sheet; the cylinders made of this sheet were tested in the first experimental series at a time when the deformation-measuring equipment was not yet developed. The values given for the 0.051-inch-thick sheet are not considered entirely reliable because of the small number (four) of creep bending tests performed. The results of the tests carried out with the 0.040- and the 0.032-inch-thick specimens appear satisfactory.

It is somewhat surprising to see the great variation in the creep constants n and λ in table 3 when the only difference among the three sets of tests is the thickness of the sheet. The reason may be the differences in the batches from which the sheets were manufactured, in the manufacturing processes the sheets underwent before delivery to the laboratory, and in the amount of cold-work to which they were subjected in the laboratory when the cylindrical shells were made out of flat sheet. Certainly the forming operation was more severe for the 0.051-inch-thick sheet than for the 0.032-inch-thick sheet when they were rolled into cylinders of the same radius.

The technique of measuring the changes in the length of the vertical diameter of the cylinder at the oven temperature of 500° F was developed while the 0.032-inch-thick cylinders were tested. All the measured values were small; moreover they did not vary monotonically. Probably the development of a bulge at some distance from the measuring device had an effect upon the measurements at the location of the device. For these reasons it is not considered useful to include a plot of these values.

The most important information obtained from the experiments is that related to the failure of the specimens. Every specimen failed by buckling. At the moment of buckling the end of the loading triangle began to accelerate downward and within a few seconds it hit the jack which was about 6 inches below the original position of the loading triangle. Buckles developed at the load end in 6 specimens, in the middle of the cylinder in 8 specimens, and at the fixed end near the strongback in 19 specimens. Figures 2, 10, and 11 show three representative cylinders with the buckles in the three locations.

The collapse time is listed in table 1 and the same information is again presented in figure 12. The experimental points can be connected by smooth lines, and, although the individual points do not lie exactly on the lines, the scatter is not pronounced.

Polytechnic Institute of Brooklyn,
Brooklyn, N. Y., August 6, 1956.

REFERENCES

1. Hoff, N. J.: Buckling at High Temperature. Symposium on Structural Problems of High-Speed Flight (Aug. 20-23, 1956, College of Aero., Cranfield, England), to be pub. in Jour. R.A.S.

2. Timoshenko, S.: Theory of Elastic Stability. First ed., McGraw-Hill Book Co., Inc., 1936.

TABLE 1

EXPERIMENTAL DATA

Cylinder	Thickness, in.	Temperature, °F	Bending moment, in-lb	Time to failure, min
1	0.064	Room	186,400	Static
2	.064	500	115,000	Static
3	.064	500	114,600	0.4
4	.064	500	100,000	12.5
5	.064	500	90,100	26.5
6	.064	500	80,000	39.1
7	.064	500	75,600	64
8	.064	500	70,000	105
9	.064	500	65,200	109
10	.064	500	65,000	130
11	.064	500	63,500	166
12	.064	500	62,000	249
13	.064	500	60,500	233
14	.064	500	55,100	321
15	.051	500	114,000	Static
16	.051	500	86,800	1.0
17	.051	500	62,700	14
18	.051	500	59,400	52
19	.051	500	54,000	86
20	.051	500	48,600	130
21	.040	500	75,200	Static
22	.040	500	84,500	Static
23	.040	500	70,600	Static
24	.040	500	54,400	3
25	.040	500	51,800	11
26	.040	500	49,100	37
27	.040	500	44,800	29
28	.040	500	44,800	40
29	.040	500	41,000	75
30	.040	500	34,600	178
31	.040	500	30,200	370
32	.032	Room	52,100	Static
33	.032	500	43,700	Static
34	.032	500	48,600	Static
35	.032	500	52,300	Static
36	.032	500	37,800	7
37	.032	500	32,400	69
38	.032	500	29,600	92
39	.032	500	27,000	116
40	.032	500	24,600	269
41	.032	500	21,600	288
42	.032	500	20,500	449
43	.032	500	46,200	Static

TABLE 2

COMPARISON OF STATIC TEST RESULTS WITH ELASTIC THEORY

Cylinder	Thickness, in.	Temperature, °F	Experimental buckling moment, in-lb	Theoretical critical moment, in-lb	Ratio of experimental to theoretical moment
1	0.064	Room	186,400	378,000	0.490
2	.064	500	115,000	288,000	.399
15	.051	500	114,000	183,000	.622
21	.040	500	75,200	113,000	.668
22	.040	500	84,500	113,000	.751
23	.040	500	70,600	113,000	.627
32	.032	Room	52,100	94,600	.550
33	.032	500	43,700	72,100	.606
34	.032	500	48,600	72,100	.674
35	.032	500	52,300	72,100	.725
43	.032	500	46,200	72,100	.640

TABLE 3

STEADY CREEP CONSTANTS

Thickness of sheet, in.	n	λ, $\frac{\text{min}^{1/n}}{(\text{lb-in.})^2}$
0.051	5.8	23,800
.040	4.1	51,000
.032	3.5	79,000

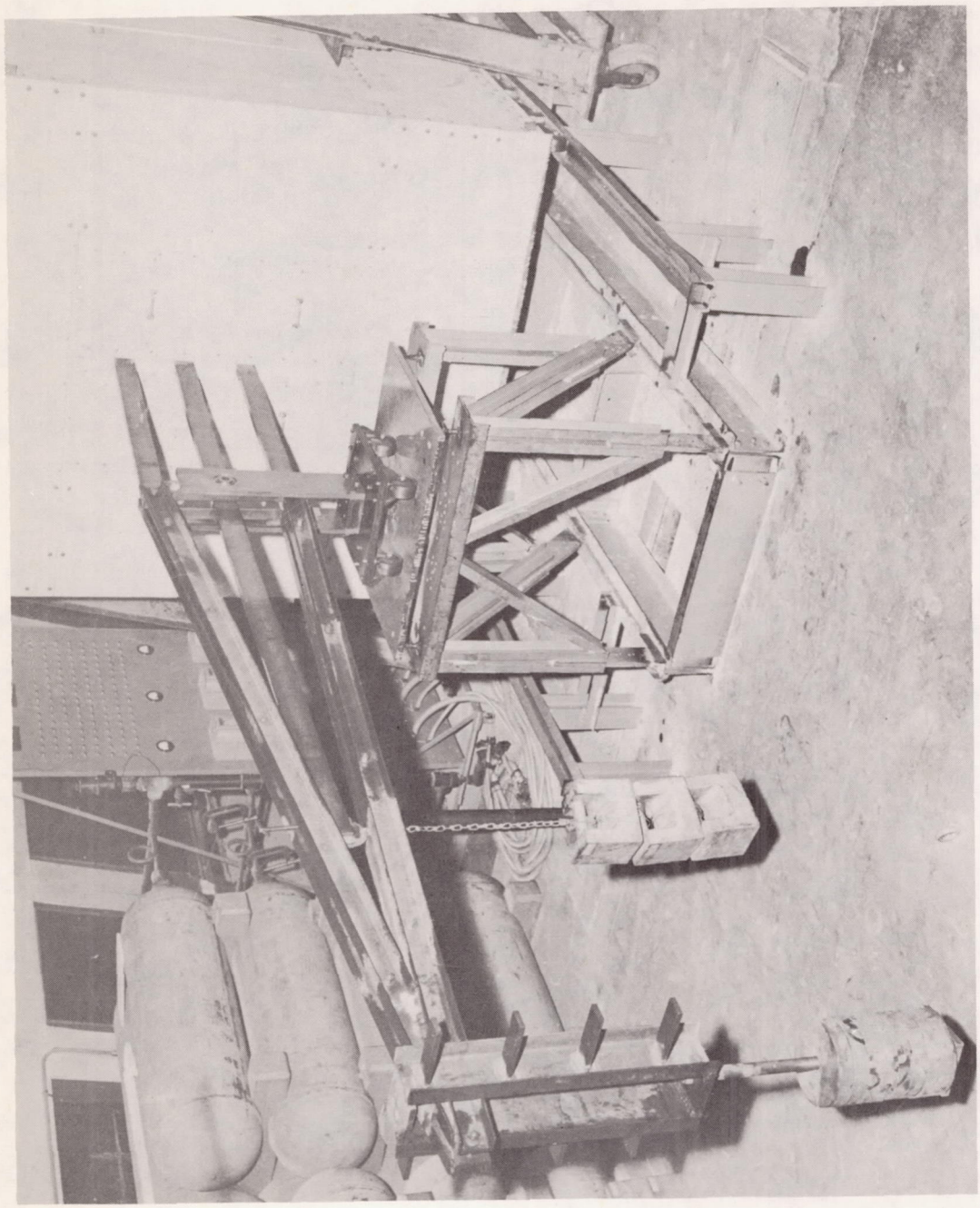

L-57-2546

Figure 1.- Loading lever and counterweight.

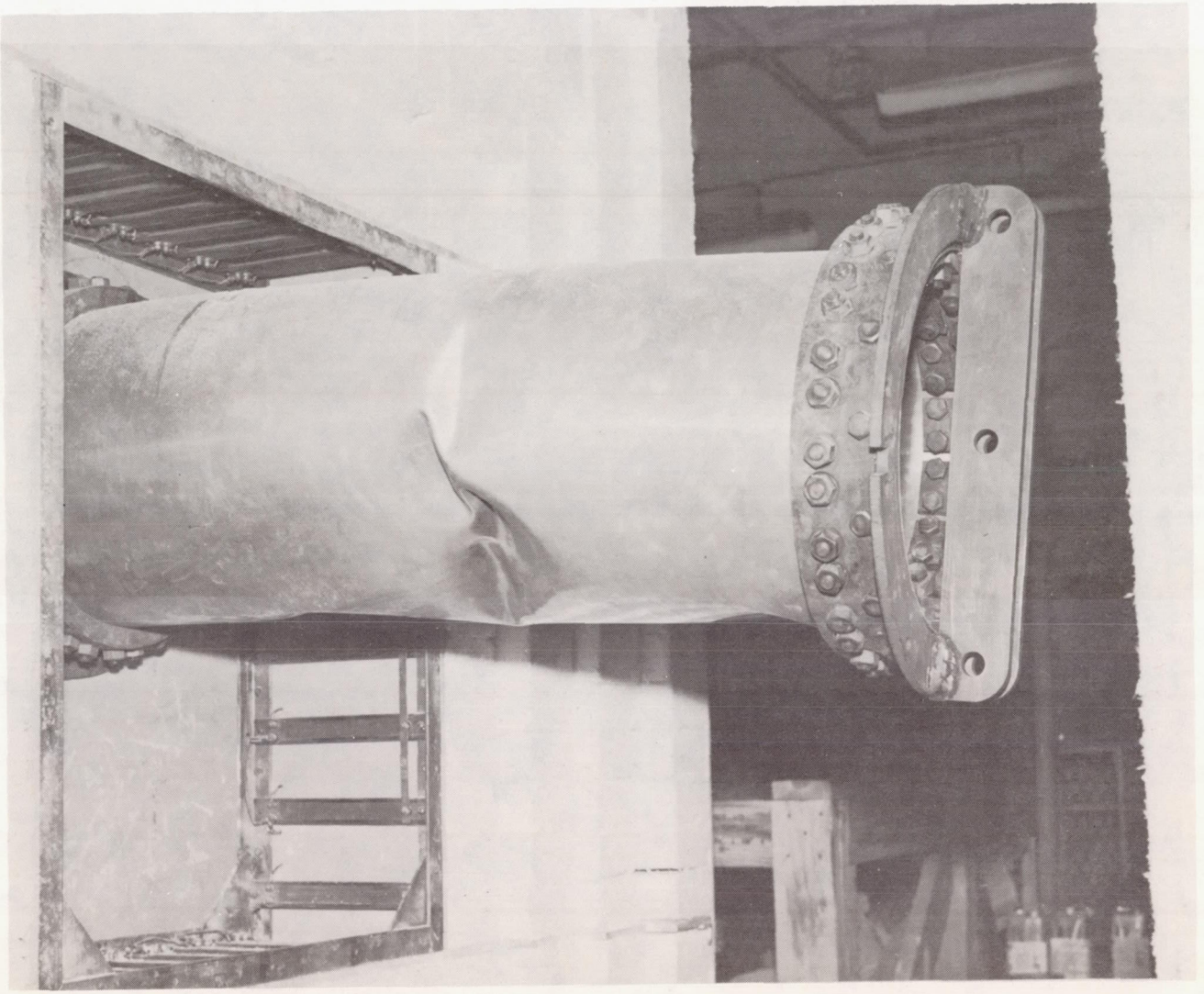

L-57-2547

Figure 2.- Cylinder 40 after failure showing attachment to loading ring.

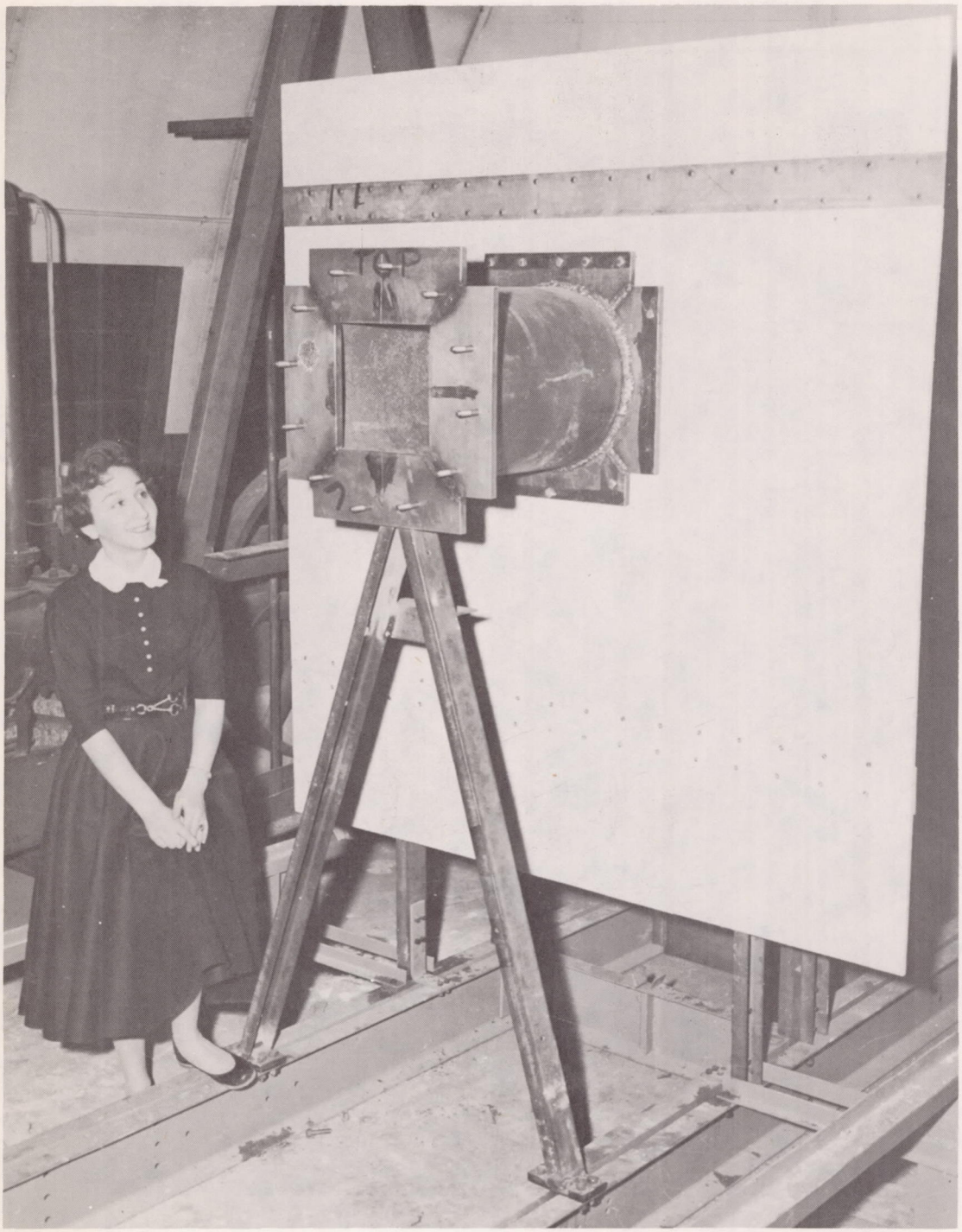

L-57-2548

Figure 3.- Strongback attachment cylinder.

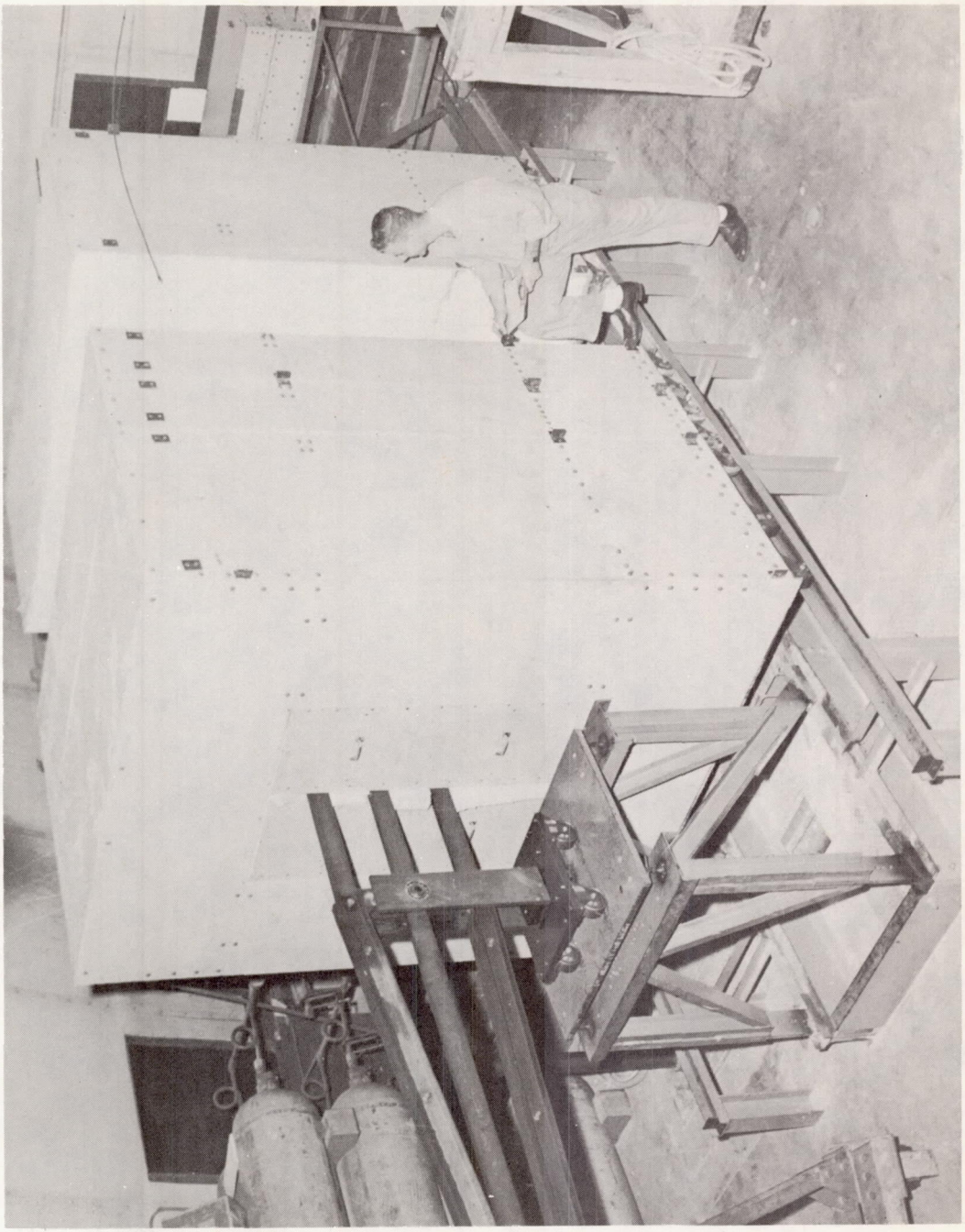

L-57-2549

Figure 4.- Overall view of oven.

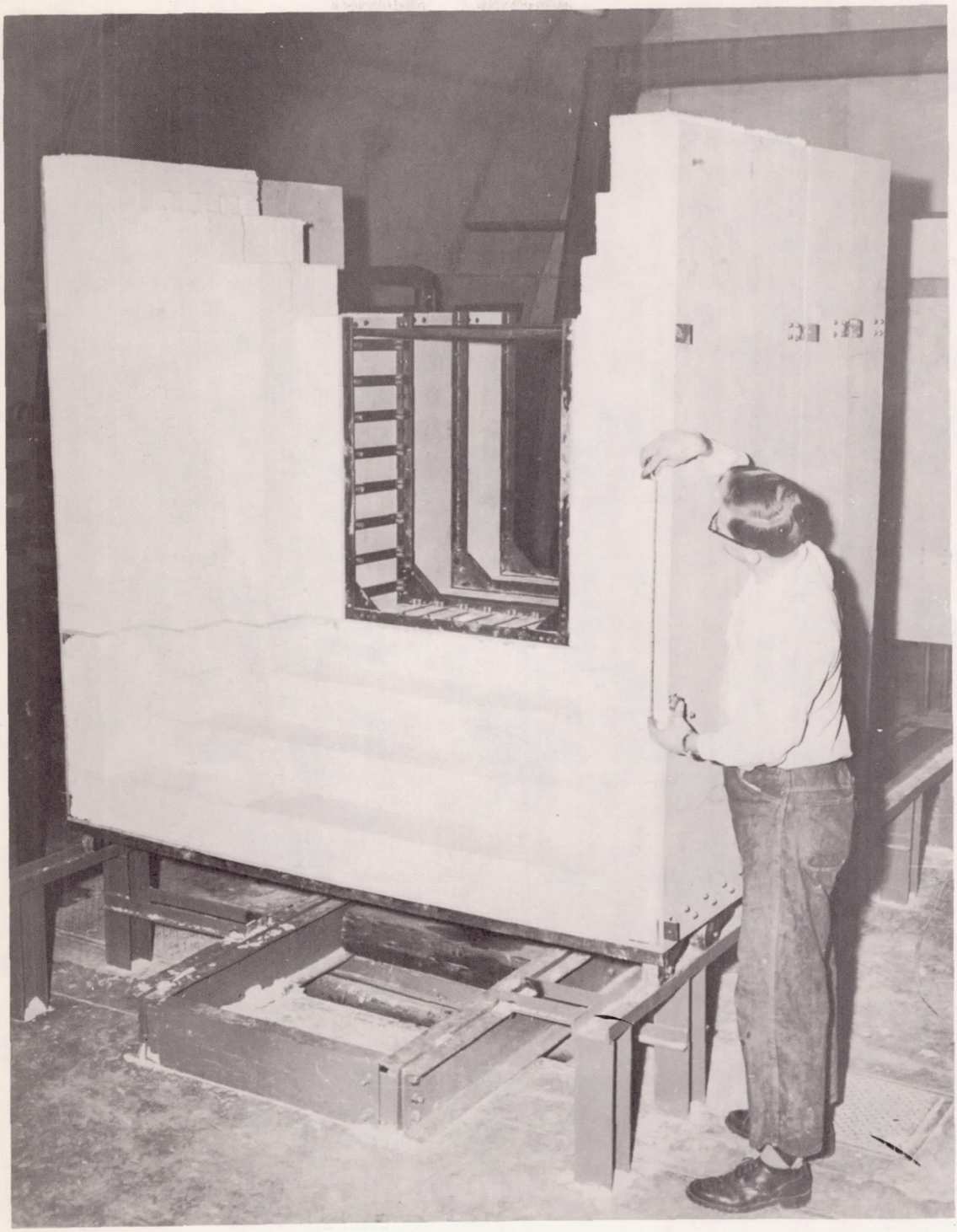

L-57-2550

Figure 5.- Partially completed section of oven.

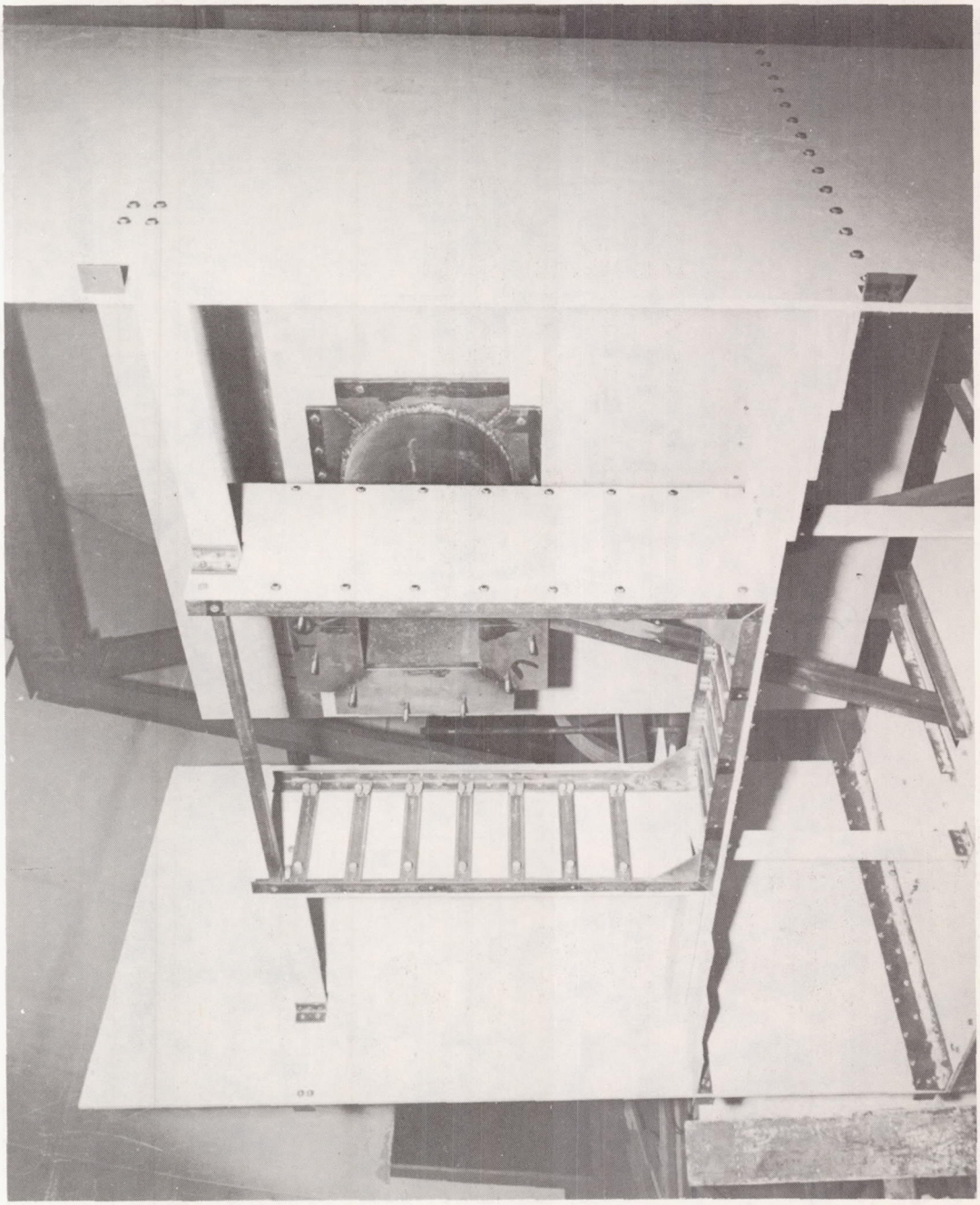

L-57-2551

Figure 6.- Skeleton of an oven section before installation of insulation.

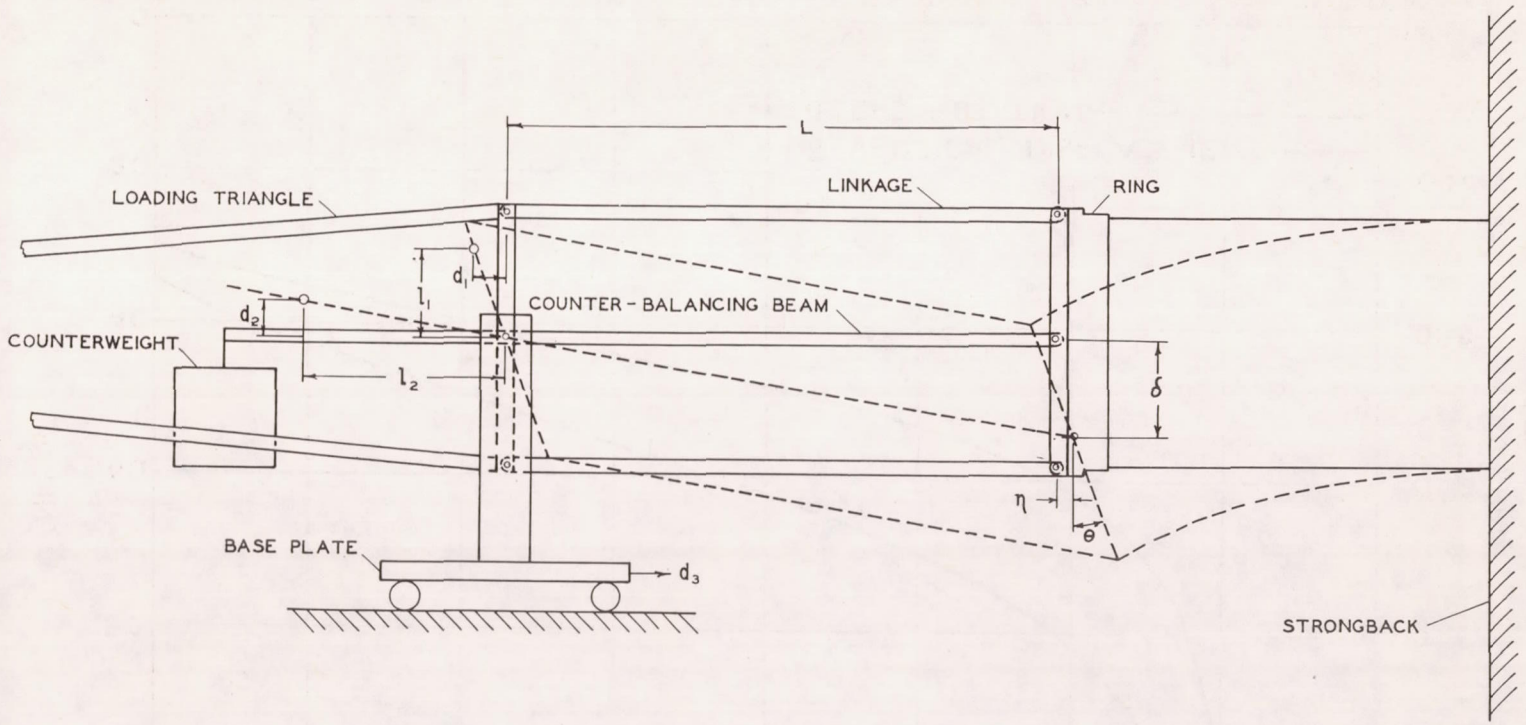

Figure 7.- Schematic drawing of equipment to measure deflections.

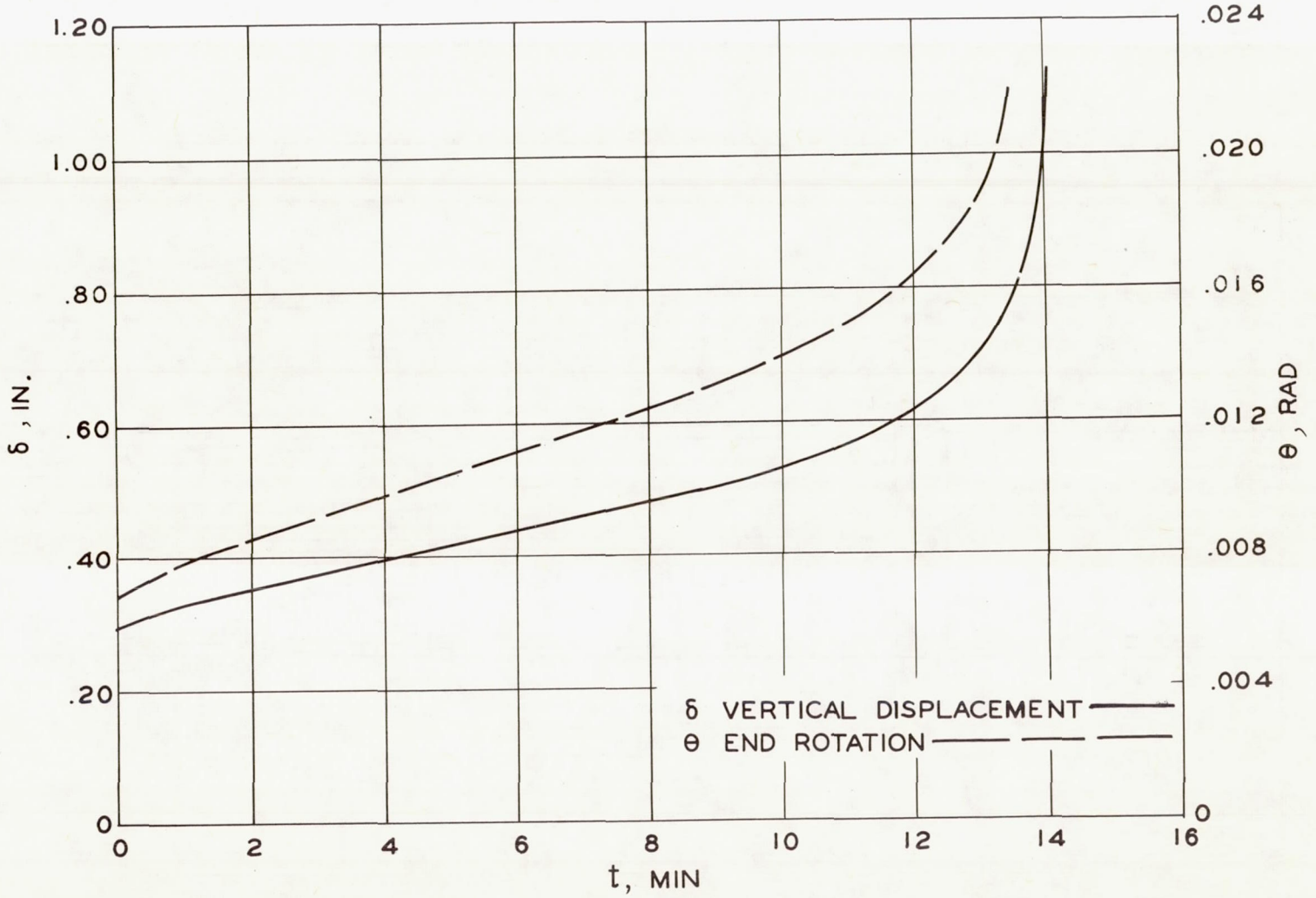

(a) Cylinder 17. Load, 580 pounds; bending moment, 62,700 inch-pounds; thickness, 0.051 inch.

Figure 8.- Time-deformation plots.

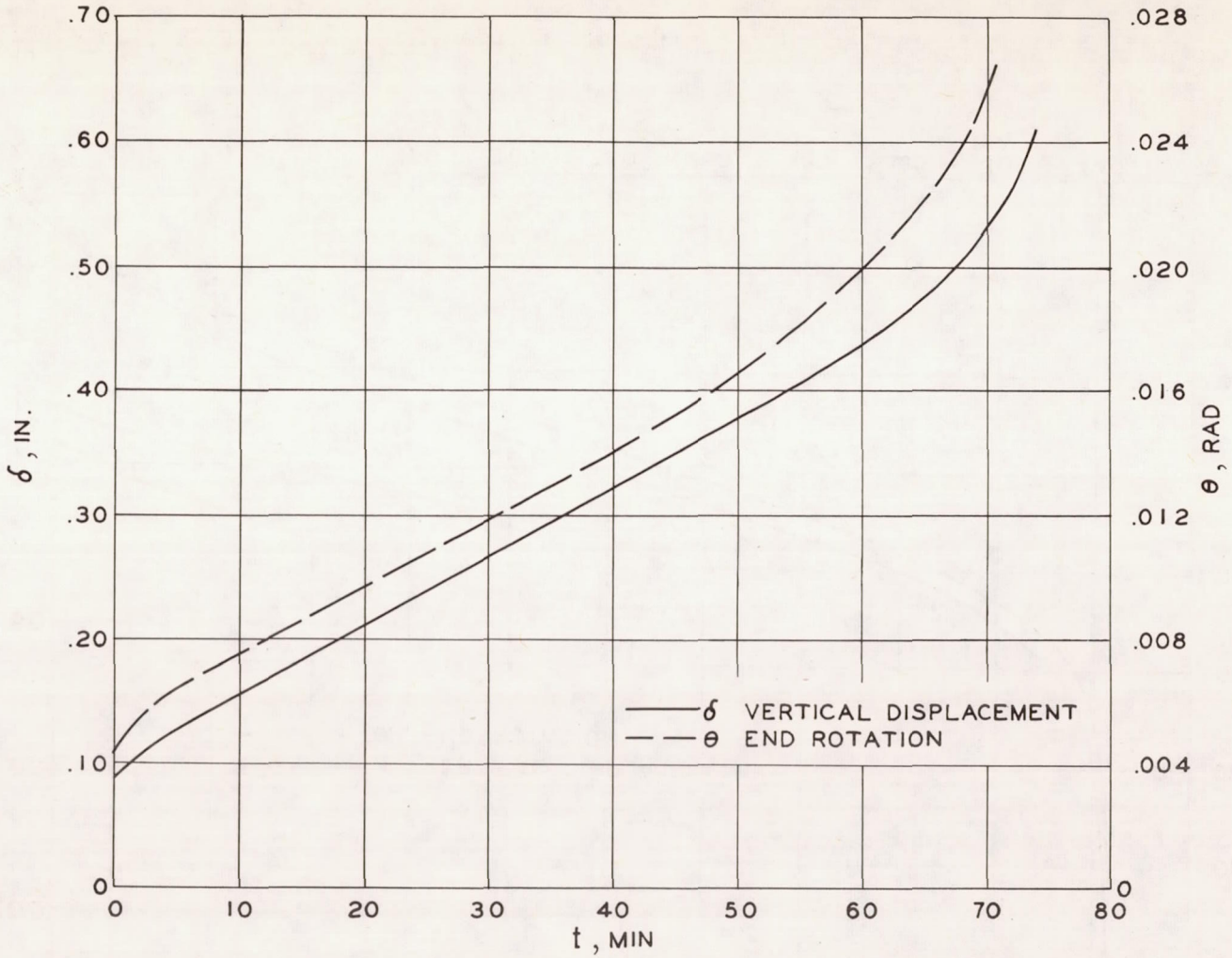

(b) Cylinder 29. Load, 380 pounds; bending moment, 41,000 inch-pounds; thickness, 0.040 inch.

Figure 8.- Continued.

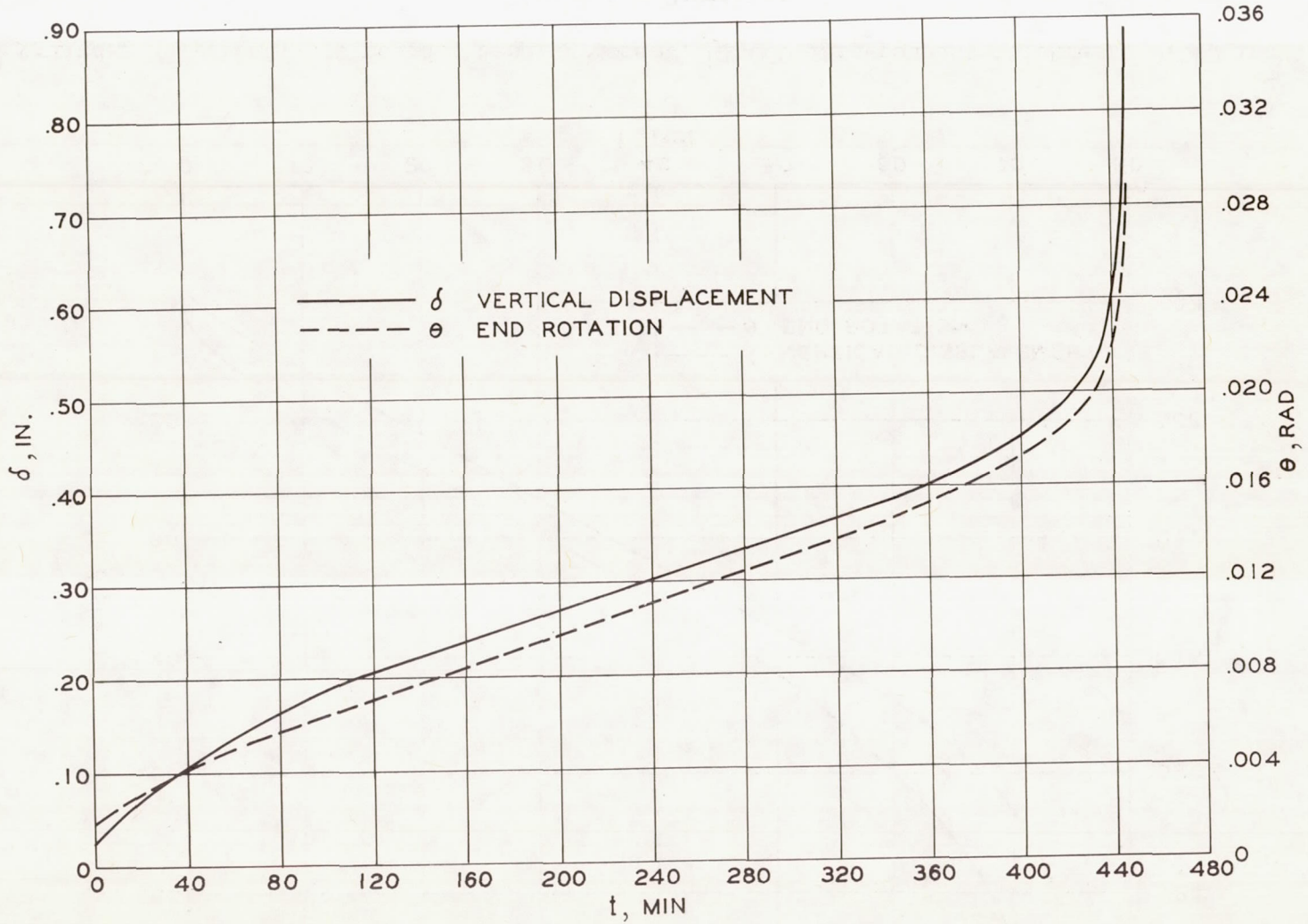

(c) Cylinder 42. Load, 190 pounds; bending moment, 20,500 inch-pounds; thickness, 0.032 inch.

Figure 8.- Concluded.

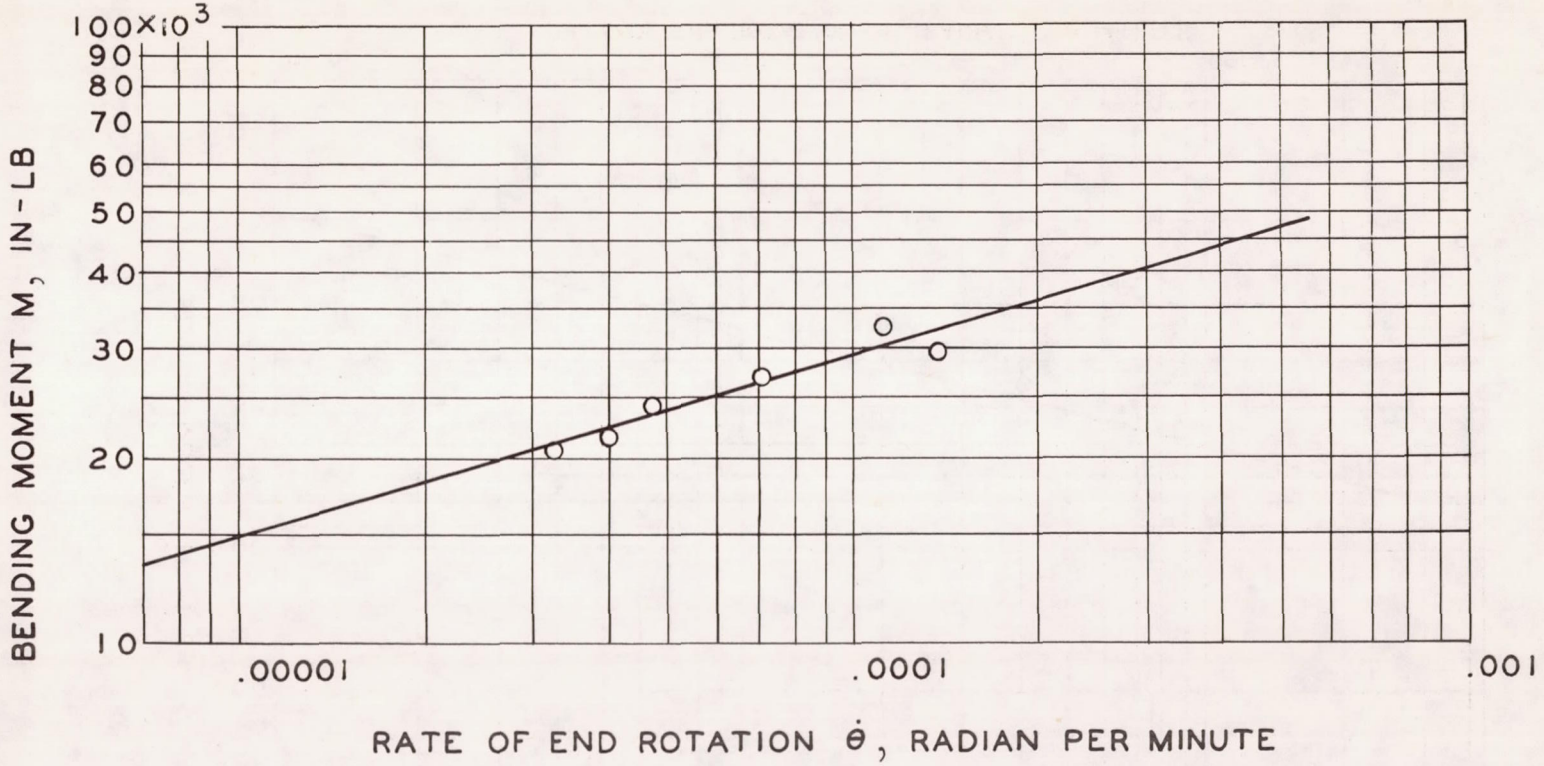

(a) h = 0.032 inch.

Figure 9.- Determination of creep constants.

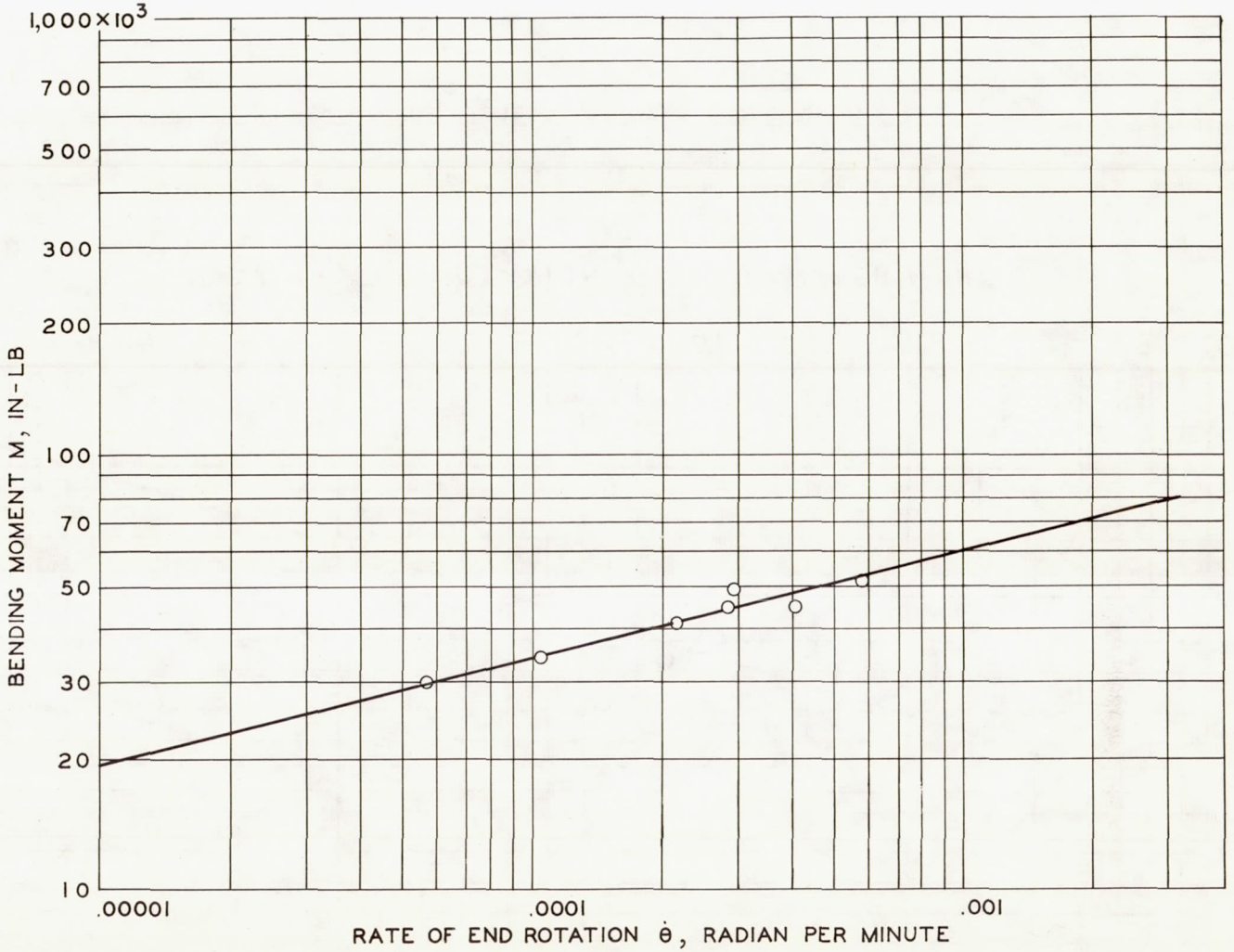

(b) h = 0.040 inch.

Figure 9.- Continued.

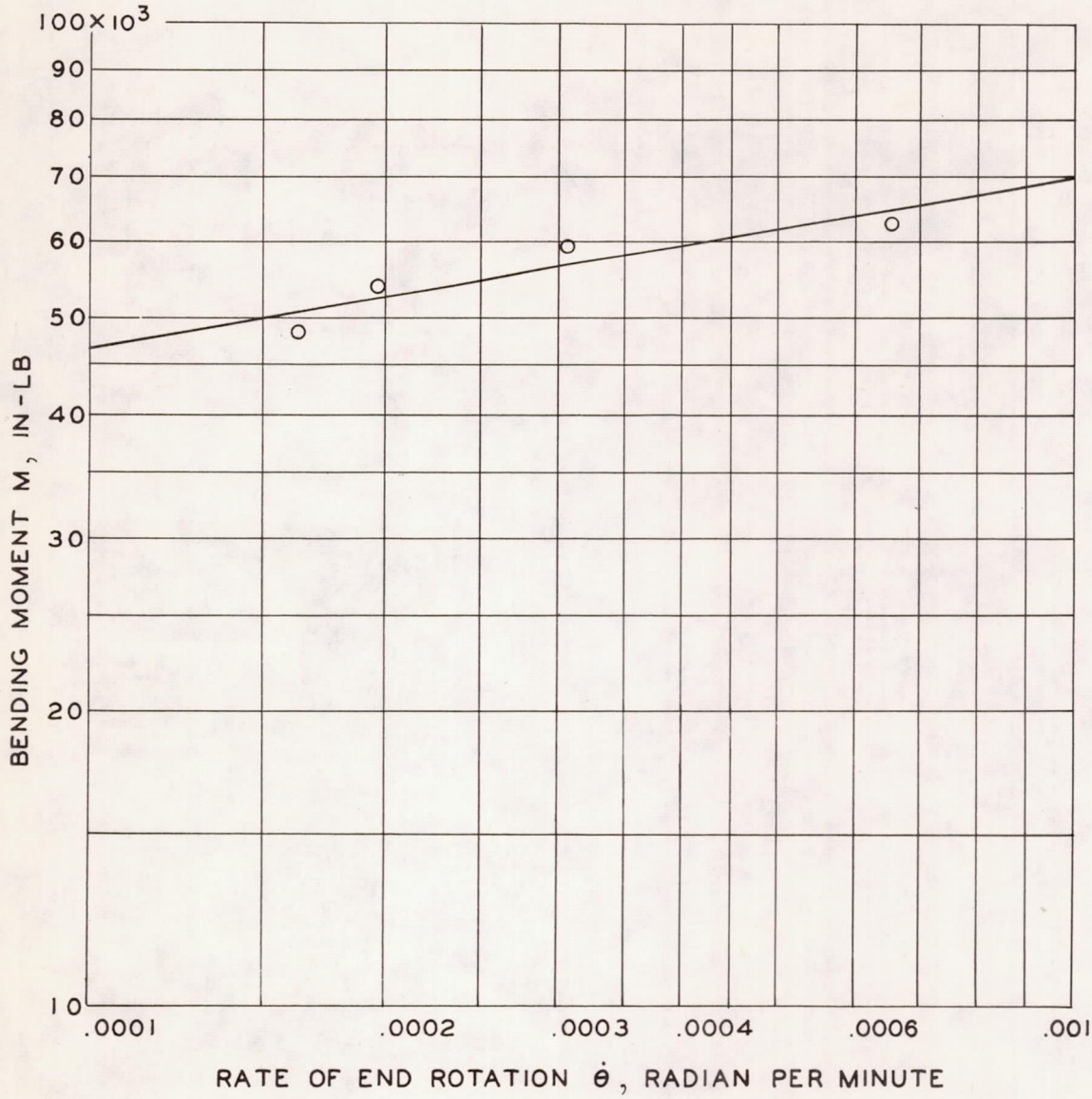

(c) h = 0.051 inch.

Figure 9.- Concluded.

L-57-2552

Figure 10.- Failure of cylinder 16. Buckle at load end.

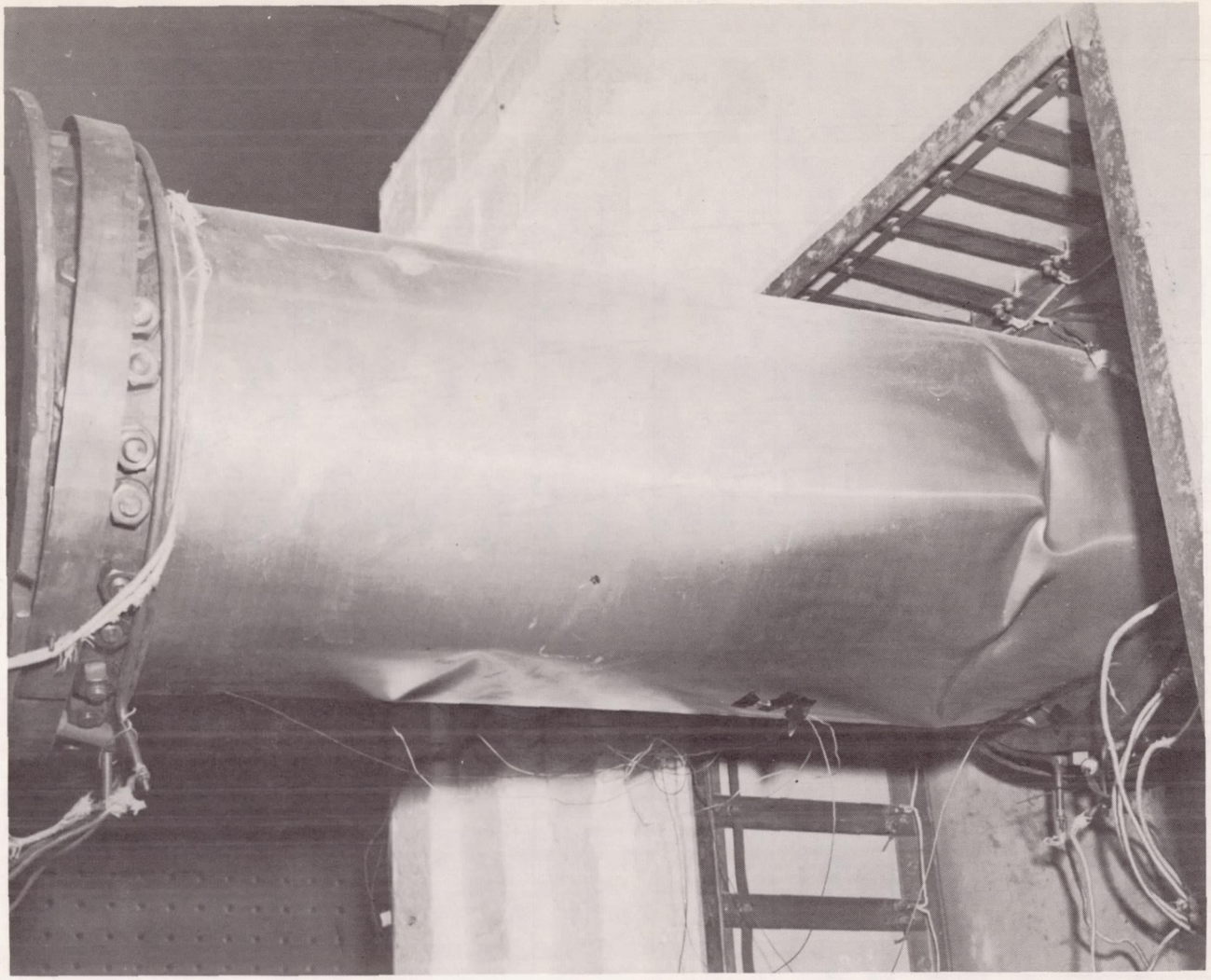

L-57-2553

Figure 11.- Failure of cylinder 25. Large buckle at fixed end and smaller one in middle.

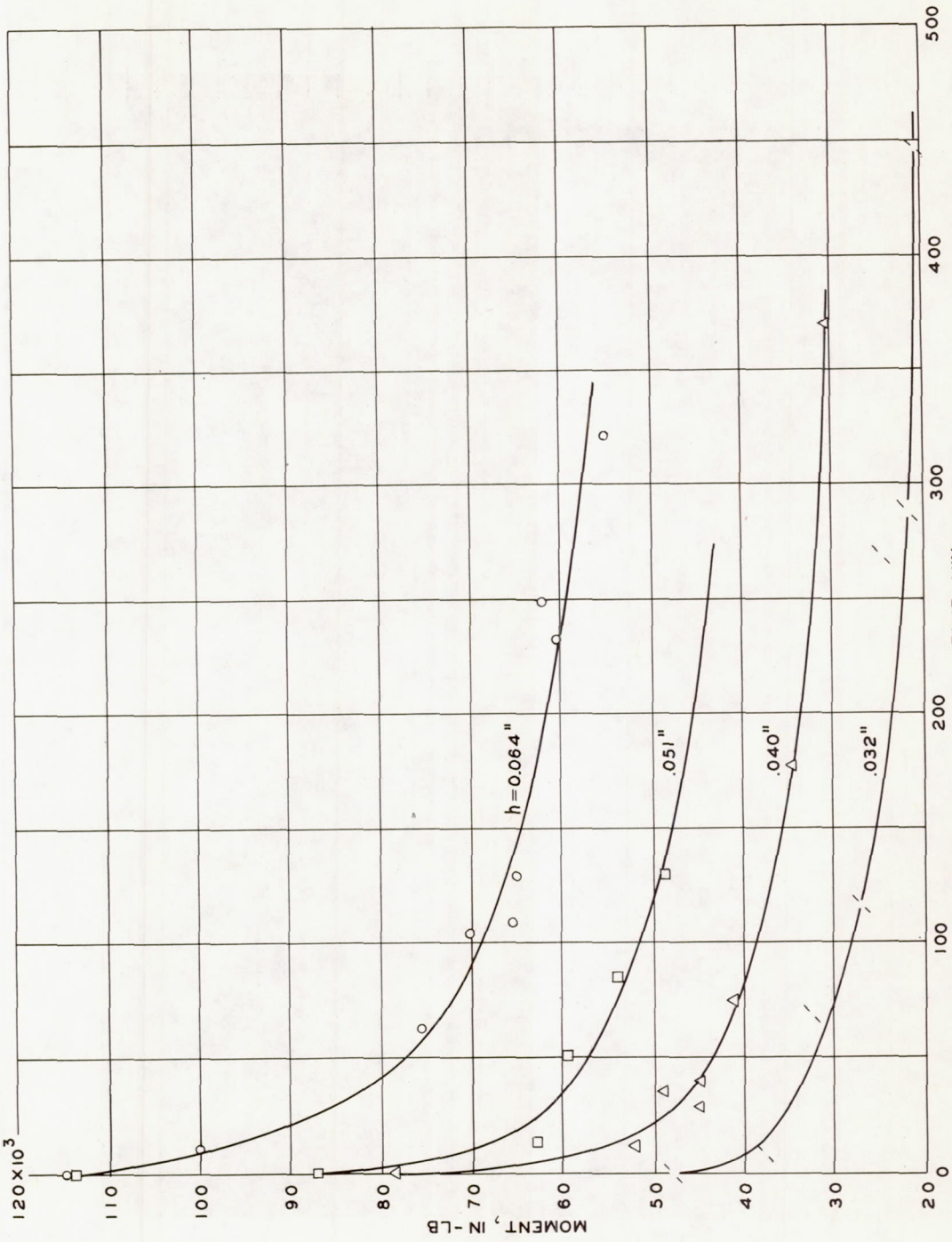

Figure 12.- Collapse time.